number of PTS groups, and 2) it possesses faster decoding convergence and lower decoder complexity. With the improved performance, better PAPR performance can be supported.

As future work, the following two aspects could be considered to further improve the decoding performance: 1) Try other optimization objectives, such as reducing the number of short-length cycles; and 2) design better algorithms so that the degrees of phase nodes are further reduced, particularly for large U.

References

[1] L. Li and D. M. Qu, "Joint decoding of LDPC code and phase factors for OFDM systems with PTS PAPR reduction," *IEEE Trans. Veh. Technol.*, vol. 62, no. 1, pp. 444–449, Jan. 2013.

[2] T. Jiang and Y. Wu, "An overview: Peak-to-average power ratio reduction techniques for OFDM signals," *IEEE Trans. Broadcast.*, vol. 54, no. 2, pp. 257–268, Jun. 2008.

[3] S. H. Muller and J. B. Huber, "OFDM with reduced peak-to-average power ratio by optimum combination of partial transmit sequences," *IEE Electron. Lett.*, vol. 33, no. 5, pp. 368–369, Feb. 1997.

[4] L. J. Cimini and N. R. Sollenberger, "Peak-to-average power ratio reduction of an OFDM signal using partial transmit sequences," *IEEE Commun. Lett.*, vol. 4, no. 3, pp. 86–88, Mar. 2000.

[5] A. D. S. Jayalath and C. Tellambura, "SLM and PTS peak-power reduction of OFDM signals without side information," *IEEE Trans. Wireless Commun.*, vol. 4, no. 5, pp. 2006–2013, Sep. 2005.

[6] O. Muta and Y. Akaiwa, "Peak power reduction method based on structure of parity-check matrix for LDPC coded OFDM transmission," in *Proc. IEEE Veh. Technol. Conf.*, Apr. 2007, pp. 2841–2845.

[7] O. Muta and Y. Akaiwa, "Weighting factor estimation method for peak power reduction based on adaptive flipping of parity bits in Turbo-coded OFDM systems," *IEEE Trans. Veh. Technol.*, vol. 57, no. 6, pp. 3551–3562, Nov. 2008.

[8] Y. C. Tsai and Y. L. Ueng, "Multiple-candidate separation for PTS-based OFDM systems by Turbo decoding," in *Proc. IEEE Veh. Technol. Conf.*, May 2010, pp. 1–5.

[9] R. G. Gallager, "Low density parity check codes," *IRE Trans. Inf. Theory*, vol. IT-8, no. 1, pp. 21–28, Jan. 1962.

[10] T. J. Richardson, A. Shokrollahi, and R. Urbanke, "Design of capacity approaching irregular low-density parity-check codes," *IEEE Trans. Inf. Theory*, vol. 47, no. 2, pp. 619–637, Feb. 2001.

[11] M. Luby, M. Mitzenmacher, A. Shokrollahi, and D. Spielman, "Improved low-density parity-check codes using irregular graphs," *IEEE Trans. Inf. Theory*, vol. 47, no. 2, pp. 585–598, Feb. 2001.

[12] *Part 16: Air interface for fixed and mobile broadband wireless access systems amendment 2: Physical and medium access control layers for combined fixed and mobile operation in licensed bands and corrigendum 1*, IEEE 802.16-2005, Feb. 2006.

Generalized Interrelay Interference Cancelation for Two-Path Successive Relaying Systems

Hao Lu, Peilin Hong, and Kaiping Xue, *Member, IEEE*

***Abstract*—This paper proposes a generalized interrelay interference cancelation (gIRIC) scheme for a two-path relay model in multisource systems. Both the sources and the relay adopt complex field network coding (CFNC) to remove the interrelay interference (IRI) caused by the two-path relay. Furthermore, we introduce two detecting modes (gIRIC-noSD and gIRIC-SD) for destination in our scheme. Two switching rules are given to select a suitable detecting mode between treating the signal of a direct link as noise (gIRIC-noSD) and utilizing the direct link to assist signal detection (gIRIC-SD). The bounds of average symbol error probability (SEP) and throughput of our scheme are derived.**

***Index Terms*—Complex field network coding (CFNC), interrelay interference (IRI), multisource, two-path relay.**

I. Introduction

Relay-based cooperative communications serves as a promising technique, which has been studied over the past decade, to extend coverage and combat channel fading in wireless networks [1], [2]. Nevertheless, due to the half-duplex nature of relay nodes, one transmission process often occupies two time slots (TSs) for the relay to receive the signal and then forward it, respectively, which results in spectral inefficiency. To overcome it, a spectrally efficient cooperative schemes named two-path successive relay was proposed in [3] and [4]. As shown in Fig. 1, at each TS, the source (S) symbol is sent to one of the relays, and the other relay forwards the symbol received from S at the previous TS. Therefore, only $(L+1)$ TSs are required to transmit L symbols from S to D, leading to an ideal throughput as high as $L/(L+1)$ symbols per source per TS (sym/S/TS). However, the two-path relay scheme results in interrelay interference (IRI) due to simultaneous transmissions of the source and the relays, which are marked in Fig. 1. Diverse schemes were proposed in [5]–[8] to deal with the IRI.

However, existing approaches have several common shortcomings. First, they only considered a single-source model. Several approaches introduced in [5]–[8] are based on binary XOR, and the others require a large number of computations. Thus, in consideration of practicability, those approaches cannot be directly extended to multisource systems. Second, most of them did not deeply discuss the effects of a direct link $(S–D)$. Due to the broadcast nature of the user terminal, it is necessary to investigate whether the interference caused by the $S–D$ link should be ignored or be exploited to assist signal detection [9]. Therefore, we are motivated to explore a new scheme for the two-path relay system. In [10], Wang and Giannakis developed complex field

Manuscript received April 26, 2013; revised July 28, 2013, November 4, 2013, and December 26, 2013; accepted January 17, 2014. Date of publication January 23, 2014; date of current version October 14, 2014. This paper was supported in part by the National Natural Science Foundation of China under Grant 61379129 and Grant 61170231 and in part by the National High-Tech Research and Development Program of China (863 Program) under Grant SS2014AA012106. The review of this paper was coordinated by Prof. Y. Zhou.

The authors are with the Information Network Laboratory, Department of Electronic Engineering and Information Science, University of Science and Technology of China, Hefei 230027, China (e-mail: lluhao@mail.ustc.edu.cn; plhong@ustc.edu.cn; kpxue@ustc.edu.cn).

Color versions of one or more of the figures in this paper are available online at http://ieeexplore.ieee.org.

Digital Object Identifier 10.1109/TVT.2014.2302309

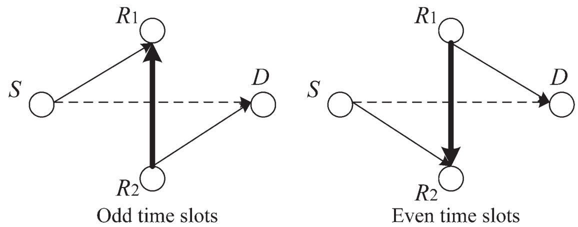

Fig. 1. Two-path relay system model. The black line arrows denote the desired signals and the bold arrows represent the IRI, whereas the dotted lines denote direct links.

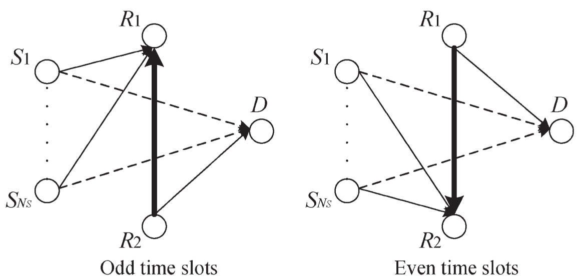

Fig. 2. (N_S, 2, 1) system model. The black line arrows denote the desired signals and the bold arrows represent the IRI, whereas the dotted lines between S_i and D denote direct links.

network coding (CFNC), which allows simultaneous transmissions of multiple sources within the same TS on the same resource blocks. In our previous work [11], we adopted physical-layer network coding [12] to deal with the IRI. Nevertheless, we did not take direct links into consideration.

Thus, in this paper, we propose a new generalized IRI cancelation (gIRIC) scheme with CFNC in the two-path successive relay system. In general, our main contributions are as follows.

- In either one-source or multisource model, we adopt CFNC at sources and relays before transmissions. We design the precoding vectors for sources and relays so that the desired symbols can be separated from the IRI through maximum likelihood (ML) detection at the receiver.
- We introduce two switching strategies for destination to select a suitable detecting mode between treating an S–D link as noise (gIRIC-noSD) and utilizing a direct link to assist signal detection (gIRIC-SD).

Notations: $(\cdot)^T$ is the transpose, $(\cdot)^*$ is the conjugation, $\mathcal{CN}(0, \sigma^2)$ is the circular symmetric complex Gaussian distribution with zero mean and variance σ^2, $\hat{x}$ is the estimation of x, and $Q(x) = 1/\sqrt{2\pi}\int_x^\infty \exp(-t^2/2)\, dt$ is the Gaussian tail function.

II. System Model

As shown in Fig. 2, this paper considers a two-path relay cooperative system that consists of N_S sources $S_1, \ldots, S_{N_S}$, two relays (R_1, R_2), and one destination D. CFNC makes it possible for sources to broadcast symbols within the same TS after symbol-level operations at the physical layer. By deploying CFNC, a cooperative network with N_S sources achieves an ideal throughput as high as 1/2 sym/S/TS [10]. Thus, we introduce CFNC into our system to distinguish source symbols and the IRI. Each source S_i broadcasts its own modulated symbols $x_i[k]$, multiplied by the precoding factor, at TS k ($k = 1, \ldots, L$), where L is the frame length. Two relay nodes, operating in the half-duplex mode and equipped with a single antenna, take turns to demodulate-and-forward the received symbol to the destination. Assuming slow flat fading, the channel coefficients between S_i and R_m, S_i and D, R_1 and R_2, R_m and D, which are represented by $h_{S_iR_m}$, h_{S_iD}, h_{12}, and h_{R_mD} ($i = 1, 2, \ldots, N_S$ and $m = 1, 2$), respectively, are modeled as zero-mean complex Gaussian random variables with finite variances $\mu_{S_iR_m}$, μ_{S_iD}, μ_{12}, and μ_{R_mD}. A channel coefficient between R_1 and R_2 satisfies channel reciprocity (i.e., $h_{12} = h_{21}$). All channel coefficients are supposed to remain constant within one frame time and vary independently from frame to frame. Regardless of environmental interference from other nodes in the network, we focus on the IRI at relay and the collisions at D. The corresponding channel noise w_{R_m} and w_D at R_m and D are assumed to be additive complex white Gaussian noise with zero mean and variance $N_0/2$. For simplicity, we allocate equal transmit power among sources and relays. Let $\mathbf{x}[k] = [x_1[k], x_2[k], \ldots, x_{N_S}[k]]^T$ denote the symbols sent by sources at TS k and $\mathbf{x}_r[k] = [\hat{x}_1[k], \hat{x}_2[k], \ldots, \hat{x}_{N_S}[k]]^T$ be the estimation of $\mathbf{x}[k]$ by relay at TS k.

III. Proposed Scheme

The core idea of CFNC [10] is to establish a one-to-one mapping between $\mathbf{x} = [x_1, x_2, \ldots, x_N]^T$ and $\Theta^T\mathbf{x}$, where $\Theta^T = [\theta_1, \theta_2, \ldots, \theta_N]$. The design of Θ^T is supposed to satisfy $\Theta^T\mathbf{x} \neq \Theta^T\mathbf{x}'$ if $\mathbf{x} \neq \mathbf{x}'$, where x'_i in $\mathbf{x}'$ is drawn from the same finite alphabet set as x_i in $\mathbf{x}$. CFNC allows simultaneous transmissions of N sources (the received symbol is $y_D = \Theta^T\mathbf{H}_{SD}\mathbf{x} + n_{SD}$, where $\mathbf{H}_{SD} = \mathrm{diag}(h_{S_1D}, \ldots, h_{S_ND})$) Then, ML detection (i.e., $\hat{\mathbf{x}} = \arg\min_{\mathbf{x}} \|y_D - \Theta^T\mathbf{H}_{SD}\mathbf{x}\|^2$) is performed at the destination to recover each source's symbol (for details, see [10]). In our system, since the signal forwarded by the relay is the superposition of N_S estimated symbols from N_S sources, we model the relay as "virtual" N_S transmitters. Thus, N_S sources, together with one of the relays, can be equivalent to a "virtual" ($2N_S$-source, 2-destination) transmission model. Therefore, we adopt $\Theta^T = [\theta_1, \theta_2, \ldots, \theta_{2N_S}]$, the design of which is based on a linear complex field encoder introduced in [10, Sec. III]. Let $\Theta_{(1)}^T = [\theta_1, \theta_2, \ldots, \theta_{N_S}]$ and $\Theta_{(2)}^T = [\theta_{N_S+1}, \theta_{N_S+2}, \ldots, \theta_{2N_S}]$. Without losing generality, we assume that, at each odd TS, original symbols from sources are multiplied by $\Theta_{(1)}^T$ and sent to R_1. Simultaneously, R_2 forwards the previously received symbols, multiplied by $\Theta_{(2)}^T$. While at each even TS, original symbols from sources are multiplied by $\Theta_{(2)}^T$ and sent to R_2. Simultaneously, R_1 forwards the previously received symbol, multiplied by $\Theta_{(1)}^T$.

Our proposed gIRIC scheme consists of two detecting modes: treating the S–D link as noise and utilizing the direct link to assist signal detection. We will separately detail both of them.

A. gIRIC for (N_S, 2, 1) Model, Ignoring S–D Link

Odd TS $2n-1 (n = 2, 3, \ldots, \lfloor L+1/2 \rfloor)$: S_i transmits its symbol as $\theta_i x_i[2n-1]$. Simultaneously, R_2 forwards $\Theta_{(2)}^T\hat{\mathbf{x}}_r[2n-2]$, where $\hat{\mathbf{x}}_r[2n-2] = [\hat{x}_1[2n-2], \hat{x}_2[2n-2], \ldots, \hat{x}_{N_S}[2n-2]]$ are the estimates of the received symbols at the previous TS. Under the assumption that symbol timing and carrier-phase synchronization have been established, the received signals by R and D are, respectively, given by

$$y_{R_1}[2n-1] = \Theta_{(1)}^T\mathbf{H}_{SR_1}\mathbf{x}[2n-1] + h_{12}\Theta_{(2)}^T\hat{\mathbf{x}}_r[2n-2] + w_{R_1}[2n-1] \quad (1)$$

$$y_D[2n-1] = h_{R_2D}\Theta_{(2)}^T\hat{\mathbf{x}}_r[2n-2] + \Theta_{(1)}^T\mathbf{H}_{SD}\mathbf{x}[2n-1] + w_D[2n-1] \quad (2)$$

where $\mathbf{H}_{SR_1} = \mathrm{diag}(h_{S_1R_1}, h_{S_2R_1}, \ldots, h_{S_{N_S}R_1})$, $\mathbf{H}_{SD} = \mathrm{diag}(h_{S_1D}, h_{S_2D}, \ldots, h_{S_{N_S}D})$, and $w_{R_1}[2n-1], w_D[2n-1] \sim \mathcal{CN}(0, N_0/2)$. We use subscript "$r$" to denote the symbol from relay nodes. All the symbols $(x_i[2n-1], \hat{x}_i[2n-2])$ sent by sources or relays are drawn from a finite alphabet $\mathcal{A}_x$ with cardinality $|\mathcal{A}_x|$, which is determined by the modulation mode.

TABLE I

DETAILED OPERATIONS OF THE PROPOSED gIRIC FOR THE (2, 2, 1) SYSTEM (L IS AN EVEN NUMBER). Tx: TRANSMIT; Rx: RECEIVE

TS	S_1 (Tx:)	S_2 (Tx:)	R_1	R_2	D (Rx:)
1	$\theta_1 x_1[1]$	$\theta_2 x_2[1]$	Rx: $\theta_1 x_1[1] + \theta_2 x_2[1]$		$(\theta_1 x_1[1] + \theta_2 x_2[1])$
2	$\theta_3 x_1[2]$	$\theta_4 x_2[2]$	Tx: $\theta_1 x_1[1] + \theta_2 x_2[1]$	Rx: $\theta_1 x_1[1] + \theta_2 x_2[1]$ $+\theta_3 x_1[2] + \theta_4 x_2[2]$	$\theta_1 x_1[1] + \theta_2 x_2[1] + (\theta_3 x_1[2] + \theta_4 x_2[2])$
3	$\theta_1 x_1[3]$	$\theta_2 x_2[3]$	Rx: $\theta_1 x_1[3] + \theta_2 x_2[3]$ $+\theta_3 x_1[2] + \theta_4 x_2[2]$	Tx: $\theta_3 x_1[2] + \theta_4 x_2[2]$	$\theta_3 x_1[2] + \theta_4 x_2[2] + (\theta_1 x_1[3] + \theta_2 x_2[3])$
4	$\theta_3 x_1[4]$	$\theta_4 x_2[4]$	Tx: $\theta_1 x_1[3] + \theta_2 x_2[3]$	Rx: $\theta_1 x_1[3] + \theta_2 x_2[3]$ $+\theta_3 x_1[4] + \theta_4 x_2[4]$	$\theta_1 x_1[3] + \theta_2 x_2[3] + (\theta_3 x_1[4] + \theta_4 x_2[4])$
$\vdots$	$\vdots$	$\vdots$	$\vdots$	$\vdots$	$\vdots$
L+1	-	-	-	Tx: $\theta_3 x_1[L] + \theta_4 x_2[L]$	$\theta_3 x_1[L] + \theta_4 x_2[L]$

For R_1, the second part of $y_{R_1}[2n-1]$ in (1) (i.e., $h_{12}\Theta_{(2)}^T \hat{\mathbf{x}}_r[2n-2]$) is the IRI, which precludes the detection of $\mathbf{x}[2n-1]$. Owing to CFNC, R_1 is able to extract the desired $\mathbf{x}[k]$ through the ML detector as follows:

$$(\hat{\mathbf{x}}[2n-1], \hat{\mathbf{x}}_r[2n-2])_{R_1} = \arg \min_{\text{all} x_i,\, x_{r_i} \in \mathcal{A}_x} \times \left\| y_{R_1}[2n-1] - \Theta_{(1)}^T \mathbf{H}_{SR_1}\mathbf{x} - h_{12}\Theta_{(2)}^T \mathbf{x}_r \right\|^2 \quad (3)$$

where x_i is the ith element of $\mathbf{x}$, whereas x_{r_i} corresponds to $\mathbf{x}_r$. It is obvious that the IRI is separated from the desired symbols. The symbol for R_1 to forward in the next TS is $x_r[2n-1] = \Theta_{(1)}^T \hat{\mathbf{x}}[2n-1]$.

Since D regards the signal of S–D link as noise, ML detection is performed at D as

$$(\hat{\mathbf{x}}_r[2n-2])_D = \arg \min_{\text{all} x_{r_i} \in \mathcal{A}_x} \left\| y_D[2n-1] - h_{R_2D}\Theta_{(2)}^T \mathbf{x}_r \right\|^2. \quad (4)$$

Since $\hat{\mathbf{x}}_r[2n-2]$ is the estimation of the received symbol at R_2 at the previous TS (i.e., $\mathbf{x}[2n-2]$), the original $(2n-2)^{\text{th}}$ symbols of N_S sources are recovered after two-hop transmissions.

Even TS $2n\,(n = 1, 2, \ldots, \lfloor L/2 \rfloor)$. S_i transmits its symbol as $\theta_{i+N_S} x_i[2n]$. Simultaneously, R_1 forwards $\Theta_{(1)}^T \hat{\mathbf{x}}_r[2n-1]$. R_2 and D receive the signals. Then, the input/output relationships are

$$y_{R_2}[2n] = \Theta_{(2)}^T \mathbf{H}_{SR_2}\mathbf{x}[2n] + h_{12}\Theta_{(1)}^T \hat{\mathbf{x}}_r[2n-1] + w_{R_2}[2n] \quad (5)$$

$$y_D[2n] = h_{R_1D}\Theta_{(1)}^T \hat{\mathbf{x}}_r[2n-1] + \Theta_{(2)}^T \mathbf{H}_{SD}\mathbf{x}[2n] + w_D[2n]. \quad (6)$$

Similar to what R_1 operates at TS $2n-1$, R_2 can extracts $\mathbf{x}[2n]$ through the ML detector. Still regarding the signal of S–D link as noise, the original $(2n-1)^{\text{th}}$ symbols of the sources are recovered at D.

To show clearly the entire procedure, we take a (2, 2, 1) system as an example and summarize the detailed operations of our gIRIC scheme within each TS in Table I, regardless of channel coefficients and noise. $N_S = 2$ results in $\Theta^T = [\theta_1, \theta_2, \theta_3, \theta_4]$ and $\Theta_{(1)}^T = [\theta_1, \theta_2]$, $\Theta_{(2)}^T = [\theta_3, \theta_4]$. At each odd TS, $\Theta_{(1)}^T$ is the precoding vector for sources, and $\Theta_{(2)}^T$ corresponds to the symbol sent by R_2. While at each even TS, the system operates in the opposite way. Therefore, only $L+1$ TSs are occupied to finish $L \times 2$ symbols' transmissions. In addition, by employing CFNC, IRI can be removed at relay nodes.

The items encapsulated in parenthesis in Table I are treated as noise at D. We further propose an alternative scheme that exploits such parts to assist signal detection.

B. gIRIC for (N_S, 2, 1) Model, Utilizing S–D Link

Due to simultaneous transmissions of all sources and one of the relays, the two-path relaying system not only generates the IRI but also introduces collisions at D. Most existing works on the two-path relay model assume that S–D link does not exist. However, in a practical mobile scenario, the signal strength of the S–D link is not always weak enough to be ignored. Therefore, we provide an alternative scheme to deal with the items encapsulated in parenthesis in Table I. The entire transmission procedure is still the same as that described earlier. We only need to rewrite (4) as follows:

$$(\hat{\mathbf{x}}_r[2n-2], \hat{\mathbf{x}}[2n-1])_D = \arg \min_{\text{all} x_{r_i}, x_i \in \mathcal{A}_x} \times \left\| y_D[2n-1] - h_{R_2D}\Theta_{(2)}^T \mathbf{x}_r - \Theta_{(1)}^T \mathbf{H}_{SD}\mathbf{x} \right\|^2. \quad (7)$$

For convenience, we let gIRIC-noSD represent the system that regards the signals of direct links as noise and gIRIC-SD represent the system that utilizes S–D links to assist signal detection.

IV. SWITCHING STRATEGIES BETWEEN gIRIC-noSD AND gIRIC-SD

For most scenarios, gIRIC-SD achieves better symbol error probability (SEP) behavior than that of gIRIC-noSD, particularly when the signal strength of the S–D link is sufficiently strong. However, gIRIC-SD requires much more computational complexity due to the ML detector. In addition, if the sources are far from the destination, the effect of direct links can be ignored without obvious degradation of system performance. Hence, taking into account the mobility of the sources, switching strategies are given here to exhibit a tradeoff between computational complexity and system performance.

It is obvious that, if $\sum_i |h_{S_iD}|$ is in the same order with $|h_{R_mD}|$ $(m = 1, 2)$, the received signal-to-interference-plus-noise ratio at D of gIRIC-noSD equals approximately $10\lg((|h_{R_mD}|^2 P)/(\sum_i |h_{S_iD|^2P+P_{noise}}))\approx 10\lg 1 = 0$ dB, which results in poor SEP, low channel capacity, and high outage probability. As a result, if $\sum_i |h_{S_iD}| \approx |h_{R_mD}|$, we recommend gIRIC-SD for the destination without additional computations on switching strategies. Therefore, the switching strategies introduced here are based on

$\sum_i |h_{S_iD}| \ll |h_{R_mD}|$. We particularly highlight that all channel coefficients remain constant within one frame time.

A. Mutual-Information-Based Switch

In this switching rule, we parameterize the system in terms of mutual information between sources and destination. Since the transmission of S–R_m link in gIRIC-noSD is the same as that in gIRIC-SD, we only consider the mutual information between R_m and D under the assumption that the source symbols are successfully detected by R_m. According to (2) and (4), the maximum average mutual information between $\mathbf{x}$ and y_D in gIRIC-noSD can be expressed as

$$I_{\text{no}SD} = \frac{1}{2}\sum_{m=1}^{2} \log\left(1 + \frac{|h_{R_mD}|^2 P}{N_0/2 + P\sum_{i=1}^{N_S}|h_{S_iD}|^2}\right) \quad (8)$$

where P is the transmit power of each sender. The factor 1/2 denotes that half of the sources' symbols are forwarded by R_1, whereas the others correspond to R_2. Likewise, in gIRIC-SD, we have

$$I_{SD} = \frac{1}{2}\sum_{m=1}^{2} \log\left(1 + \frac{|h_{R_mD}|^2 P + P\sum_{i=1}^{N_S}|h_{S_iD}|^2}{N_0/2}\right). \quad (9)$$

Therefore, for mutual-information-based switching, the destination chooses the detecting mode based on

$$\begin{cases} \text{gIRIC-noSD}, & \text{if } I_{\text{no}SD} + \text{bias}_1 \geq I_{SD} \\ \text{gIRIC-SD}, & \text{if } I_{\text{no}SD} + \text{bias}_1 < I_{SD} \end{cases} \quad (10)$$

where $\text{bias}_1 = \lambda_1 f_1$. bias_1 reveals the overall complexity saved by gIRIC-noSD. f_1 is a function of computational complexity. λ_1 ensures that bias_1 and mutual information are of the same order. bias_1 varies according to different system constraints. For example, if the transmission requires a high data rate, it may adopt small bias_1. Conversely, gIRIC-noSD is a suitable choice to achieve low complexity with large bias_1. The calculations of (9) and (10) only need to be performed once per $L+1$ TSs or when channel coefficients obviously change.

However, without consideration about the modulation mode and the fact that channel capacity is the theoretical bound, such mutual information-based switch is too idealistic. In practice, modulation mode plays a significant role in determining SEP behavior, which reflects the throughput under a fixed transmission rate. Consequently, we introduce a simplified SEP-based switching rule.

B. Simplified SEP-Based Switch

All symbols are delivered to D through S–R–D. The SEP at D can be expressed as

$$P_{e-\text{no}SD} = (1 - P_{e-SR})P_{e-RD} + P_{e-SR} \quad (11)$$

where P_{e-SR} represents the SEP of the S–R link, whereas P_{e-RD} corresponds to the R–D link. Both of the detecting modes share the same SEP of the S–R link. As a result, simplified SEP-based switching rule parameterizes the system only in terms of P_{e-RD}. Making use of the union bound [13], the average SEP of the R–D link for gIRIC-noSD is upper bounded by

$$P_{RD-\text{no}SD} \leq \frac{1}{2}(M^{N_S}-1)\sum_{m=1}^{2} Q\left(\frac{|h_{R_mD}|d_{\min}^{\Theta^T\mathbf{x}}}{\sqrt{2(N_0+2P\sum_{i=1}^{N_S}|h_{S_iD}|^2)}}\right) \quad (12)$$

where $d_{\min}^{\Theta^T\mathbf{x}}$ is the minimum Euclidean distance in the constellation of $\Theta_{(m)}^T\mathbf{x}$ and $M = |\mathcal{A}_x|$. To facilitate the calculation, we make another approximation based on the Chernoff bound [14]

$$P_{RD-\text{no}SD} \leq \frac{1}{2}(M^{N_S}-1)\sum_{m=1}^{2} \times \exp\left(-\frac{|h_{R_mD}|^2 d_{\min}^{2\Theta^T\mathbf{x}}}{4(N_0 + 2P\sum_{i=1}^{N_S}|h_{SD}|^2)}\right). \quad (13)$$

Likewise, for gIRIC-SD, the corresponding SEP of the R–D link is given by

$$P_{RD-SD} \leq \frac{1}{2}(M^{N_S}-1)\sum_{m=1}^{2} \exp\left(-\frac{|h_{R_mD}|^2 d_{\min}^{2\Theta^T\mathbf{x}}}{4N_0}\right). \quad (14)$$

Then, the simplified SEP-based switching rule is given as

$$\begin{cases} \text{gIRIC-noSD}, & \text{if } P_{RD-\text{no}SD} \leq P_{RD-SD} + \text{bias}_2 \\ \text{gIRIC-SD}, & \text{if } P_{RD-\text{no}SD} > P_{RD-SD} + \text{bias}_2 \end{cases} \quad (15)$$

where $\text{bias}_2 = \lambda_2 f_2$. λ_2 and f_2 play the same role as λ_1 and f_1. Since the range of SEP is different from that of mutual information, former bias_1 is no longer applicable. Thus, bias_2 is the redesign of bias_1.

C. Discussion

The selection of detecting mode is performed at D as follows.

1) When the first two symbols in a frame arrive, D measures channel coefficients via estimation from training sequences in protocol headers.
   - If channel coefficients are the same as those of the former frame, D continuously operates in the same detecting mode and continues with Step 3.
   - If $\sum_i |h_{S_iD}| \approx |h_{R_mD}|$, D directly chooses gIRIC-SD and continues with Step 3.
2) According to measured channel coefficients, D performs one of the two switching rules to determine a suitable detecting mode.
3) Based on the chosen detecting mode, D estimates the received symbols until the end of this frame or obvious changes of channel coefficients.

The mutual-information-based switch requires fewer computations, whereas the simplified SEP-based switch is consistent with practice via taking into account divers modulation constellations at a cost of more computational complexity. We provide these comparisons as the reference for choosing a switching rule between the given alternatives in Step 2.

The configurations of $\text{bias}_t (t = 1, 2)$ play a significant role in switching. Since bias_t reflects system overheads that vary in different networks and is not the focus of our paper, we will not detail its design.

V. Symbol Error Probability and Throughput Analysis

Earlier, in the simplified SEP-based switch, only the SEP of the R–D link is deduced to achieve fewer computations. Thus, here, the bounds of average end-to-end (e2e) SEP from each source to the destination and the throughput will be analyzed. Regardless of computational complexity, we focus on the gIRIC-SD detecting mode.

Let $s = \Theta_{(\bar{m})}^T \mathbf{H}_{SD}\mathbf{x} - h_{R_mD}\Theta_{(m)}^T\mathbf{x}_r$, where $(m = 1, \bar{m} = 2)$ or $(m = 2, \bar{m} = 1)$. The destination should recover the symbols from relay (i.e., $\mathbf{x}_r$). According to [11, Sec. V-A], adopting e CFNC in the multisource system, the result calculated via (14) is the SEP of s, rather than $x_{r_i} \in \mathbf{x}_\mathbf{r} (i = 1, 2, \ldots, N_S)$. To obtain an average e2e SEP from each source to the destination, we rewrite (11) as

$$P_{\text{e2e}}^* = P_{e-RD}^* + P_{e-SR}^* - P_{e-SR}^* P_{e-RD}^* \quad (16)$$

where P_{e2e}^*, P_{e-SR}^*, and P_{e-RD}^* represent the average e2e SEP of source–destination, source–relay, and relay–destination, respectively.

TABLE II
SIMULATION PARAMETERS

Parameters	Value
Modulation Mode	BPSK
Packet Size (L)	128 bits
Source number (N_S)	1/2/3
User Antenna Gain	0 dBi
Θ^T	LCF[21]
Noise Power	-174 dBm/Hz
Channel fading	Rayleigh fading

According to [11, Eq. (25)], we have

$$P^*_{e\text{-}RD} \leq \frac{1}{2N_S|\mathcal{A}_s|}\sum_{m=1}^{2}\sum_{k=1}^{N_S} k \sum_{a=1}^{|\mathcal{A}_s|}\left(\sum_{\substack{b=1,\\ \|\mathbf{x}_{r_a}-\mathbf{x}_{r_b}\|_0=k}}^{|\mathcal{A}_s|} Q\left(\frac{d_{ab}^{(s)}}{\sqrt{2N_0}}\right)\right) \quad (17)$$

where $d_{ab}^{(s)}$ denotes the Euclidean distance between s_a and s_b. $s_a = \Theta^T_{(\bar{m})}\mathbf{H}_{SD}\mathbf{x}_a - h_{R_mD}\Theta^T_{(m)}\mathbf{x}_{r_a}$ and $s_b = \Theta^T_{(\bar{m})}\mathbf{H}_{SD}\mathbf{x}_b - h_{R_mD}\Theta^T_{(m)}\mathbf{x}_{r_b}$ are two different points in the constellation of s (finite alphabet $\mathcal{A}_s$ with cardinality $|\mathcal{A}_s|$). $\|\mathbf{x}_{r_a} - \mathbf{x}_{r_b}\|_0$ indicates the number of nonzero elements of $\mathbf{x}_{r_a} - \mathbf{x}_{r_b}$.

For the source–relay link, let $z = \Theta^T_{(m)}\mathbf{H}_{SR_m}\mathbf{x} + h_{12}\Theta^T_{(\bar{m})}\mathbf{x}_r$ (the signal received by relay, regardless of noise). The relay wants to recover $\mathbf{x}$. As in the relay–destination link, P^*_{e-SR} can be calculated through the following:

$$P^*_{e-SR} \leq \frac{1}{2N_S|\mathcal{A}_z|}\sum_{m=1}^{2}\sum_{k=1}^{N_S} k \sum_{a=1}^{|\mathcal{A}_z|}\left(\sum_{\substack{b=1\\ \|\mathbf{x}_a-\mathbf{x}_b\|_0=k}}^{|\mathcal{A}_z|} Q\left(\frac{d_{ab}^{(z)}}{\sqrt{2N_0}}\right)\right). \quad (18)$$

$d_{ab}^{(z)}$ represents the Euclidean distance between z_a and z_b, where $z_a = \Theta^T_{(m)}\mathbf{H}_{SR_m}\mathbf{x}_a + h_{12}\Theta^T_{(\bar{m})}\mathbf{x}_{r_a}$, and $z_b = \Theta^T_{(m)}\mathbf{H}_{SR_m}\mathbf{x}_b + h_{12}\Theta^T_{(\bar{m})}\mathbf{x}_{r_b}$. Then, based on (17) and (18), the upper bound of the average e2e SEP from each source to the destination (P^*_{e2e}) is obtained through (16).

Here, the throughput (represented by T) is defined as the number of successfully recovered symbols by the destination per TS. Thus, the throughput of our proposed scheme is expressed as

$$T_{\text{gIRIC}} = \frac{1}{L+1}\sum_{n=2}^{L+1} N_S \times \left(1 - P_{\text{e2e}}^{(n)}\right) \quad \text{sym/TS} \quad (19)$$

where $P_{\text{e2e}}^{(n)}$ is the average e2e SEP at the destination during TS n. Since there is no IRI at TS 1 and no interference at TS $L+1$, $P_{\text{e2e}}^{(n)}$ is given by

$$P_{\text{e2e}}^{(n)} = \begin{cases} P^*_{e-RD} + P'_{e-SR} - P'_{e-SR}P^*_{e-RD}, & n = 2 \\ P^*_{\text{e2e}}, & n \in [3, L] \\ P'_{e-RD} + P^*_{e-SR} - P^*_{e-SR}P'_{e-RD}, & n = L+1 \end{cases} \quad (20)$$

where P'_{e-SR} and P'_{e-RD} are the average e2e SEPs in the case of no IRI at relay and no collision at destination, respectively. With large L, we have $T_{\text{gIRIC}} \approx N_S(1 - P^*_{\text{e2e}})$. With the increase in SNR, the upper bound of T_{gIRIC} is N_S sym/TS. The given derivations are based on gIRCI-SD. The analysis on gIRIC-noSD is analogous to that of gIRIC-SD.

VI. SIMULATION

A. Simulation Setup

Here, the SEP behaviors of our proposed scheme are investigated through Monte Carlo simulations. Some primary simulation parameters are presented in Table II. In addition, we set $h_{S_iR_m}$, h_{12}, and $h_{R_mD} \sim \mathcal{CN}(0, 1)$. Let $\gamma_{S_iR} = \gamma_{RD} = \gamma_{12} = \gamma = (P/N_0/2)$, denoting the notation "SNR" in Figs. 3–5. We assume $E\{|h_{S_iD}|^2\} \in \{0.1, \sqrt{0.1}\}$ to simulate different positions of sources, corresponding to $\gamma_{S_iD} = \gamma - 10$ dB and $\gamma_{S_iD} = \gamma - 5$ dB, respectively.

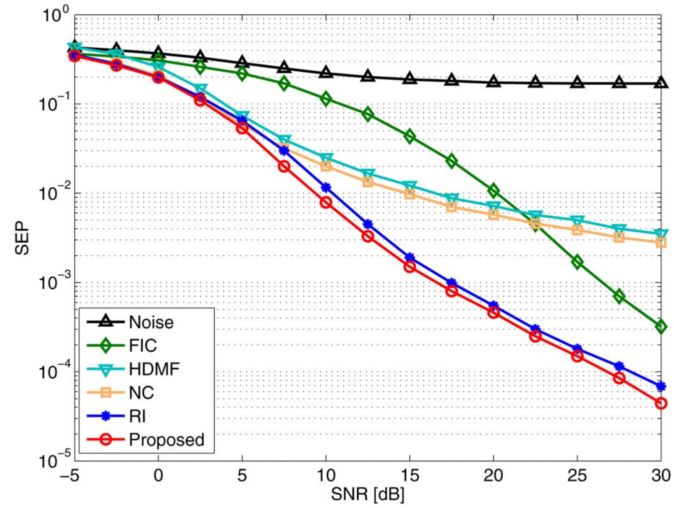

Fig. 3. SEP comparisons in the (1, 2, 1) system. $\gamma_{SD} = \gamma - 5$ dB.

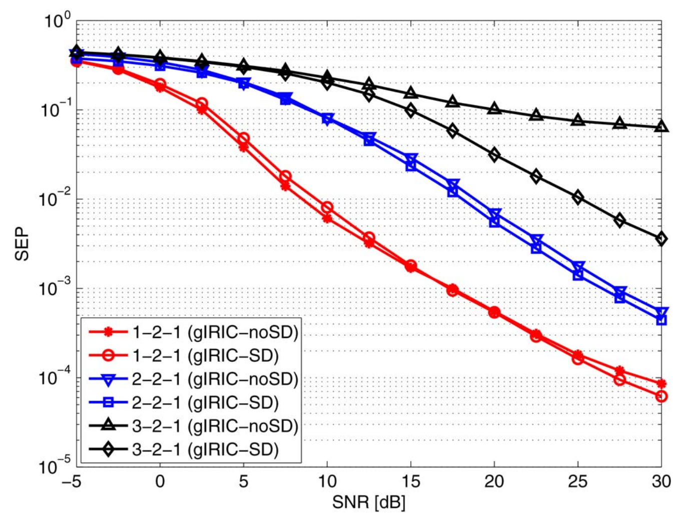

Fig. 4. SEP comparisons between the proposed gIRIC-noSD and gIRIC-SD in the (N_S, 2, 1) system. $\gamma_{S_iD} = \gamma - 10$ dB.

For comparison, we choose several existing strategies as the benchmarks. First, the scheme that treats the interrelay signals as noise, labeled as "Noise," is considered to demonstrate the necessity of removing IRI. Then, the schemes proposed in [5]–[8] are labeled as "NC," "FIC," "RI," and "HDMF," respectively. We label our proposed scheme as "Proposed" or "gIRIC."

B. Results and Discussions

First, we compare the SEP performance of our scheme with those of existing strategies in the (1, 2, 1) system, as shown in Fig. 3. Since we mainly aim at verifying the lower SEP achieved by the proposed scheme, D adopts gIRIC-SD. Based on the fact that these benchmarks, except FIC, do not take the S–D link into consideration, our gIRIC achieves the best SEP behavior throughout the range of SNR. Among all benchmarks, RI exploits the orthogonality of the inphase and quadrature-phase components of the symbol to distinguish the information and interference, which is similar to our gIRIC when $\theta_1 = 1$ and $\theta_2 = j$. FIC also considers the effect of the S–D link, which leads to a faster decrease in SEP within a high SNR.

Second, we compare the performance between gIRIC-noSD and gIRIC-SD in (N_S, 2, 1) systems ($N_S = 1/2/3$). In Fig. 4, we set

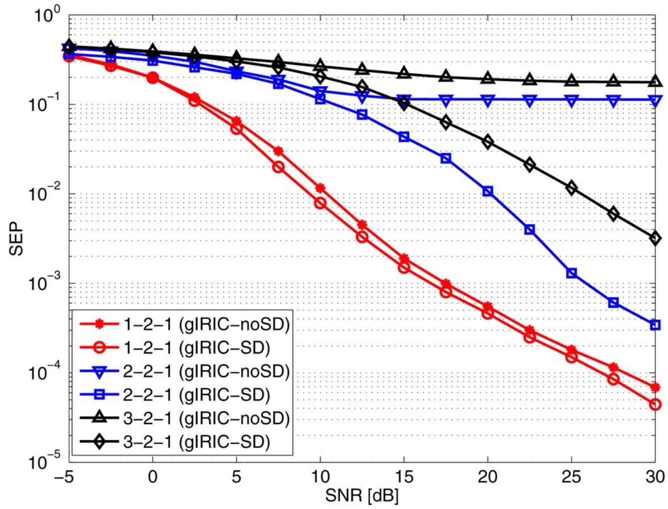

Fig. 5. SEP comparisons between the proposed gIRIC-noSD and gIRIC-SD in the $(N_S, 2, 1)$ system. $\gamma_{S_iD} = \gamma - 5$ dB.

$\gamma_{S_iD} = \gamma - 10$ dB, which suggests that sources are far away from the destination. Under this assumption, the signal strength of direct link is so weak that the SEP behavior of gIRIC-noSD is similar to that of gIRIC-SD. Under a low SNR region, we recommend gIRIC-noSD since both of the detecting modes achieve similar performance. Although each $|h_{S_iD}|$ is small, the value of $\sum_{i=1}^{N_S} |h_{S_iD}|^2$ increases with the growth of N_S. Thus, at the high SNR region, gIRIC-noSD substantially degrades the SEP in the (3, 2, 1) system. Taking the mobility of the sources into account, we change γ_{S_iD}. The SEP of gIRIC-noSD in either (2, 2, 1) or (3, 2, 1) system deteriorates due to $\gamma_{S_iD} = \gamma - 5$ dB, as shown in Fig. 5, which shows the necessity of performing detecting modes' selection at D.

VII. Conclusion

In this paper, we have proposed a new scheme named gIRIC in a two-path relay system. In gIRIC, CFNC and ML detection are performed to separate each source symbol and the IRI. Taking direct links into consideration, we introduced two switching rules for destination to select a suitable detecting mode between gIRIC-noSD and gIRIC-SD. Then, the bounds of average e2e SEP and throughput were derived. In addition, numerical simulation results verified the SEP improvement of gIRIC and the effects of direct links.

Acknowledgment

The authors would like to thank the editor and anonymous reviewers for their valuable suggestions that significantly improve the quality of this paper.

References

[1] J. N. Laneman and G. W. Wornell, "Distributed space-time coded protocols for exploiting cooperative diversity in wireless networks," *IEEE Trans. Inf. Theory*, vol. 49, no. 10, pp. 2415–2425, Oct. 2003.
[2] J. N. Laneman, D. N. C. Tse, and G. W. Wornell, "Cooperative diversity in wireless networks: Efficient protocols and outage behavior," *IEEE Trans. Inf. Theory*, vol. 50, no. 12, pp. 3062–3080, Dec. 2004.
[3] T. Oechtering and A. Sezgin, "A new cooperative transmission scheme using the space-time delay code," in *Proc. ITG Workshop Smart Antenna*, Mar. 18–19, 2004, pp. 41–48.
[4] A. Ribeiro, X. Cai, and G. B. Giannakis, "Opportunistic multipath for bandwidth-efficient cooperative networking," in *Proc. Int. Conf. Acoust., Speech Signal Process.*, May 2004, pp. 549–552.
[5] C. Luo, Y. Gong, and F.-C. Zheng, "Interference cancellation in two-path successive relay system with network coding," in *Proc. Pers., Indoor, Mobile Radio Commun.*, Sep. 26–30, 2010, pp. 465–469.
[6] C. Luo, Y. Gong, and F.-C. Zheng, "Full interference cancellation for two-path relay cooperative networks," *IEEE Trans. Veh. Technol.*, vol. 60, no. 1, pp. 343–347, Jan. 2011.
[7] L. Sun, T. Zhang, and H. Niu, "Inter-relay interference in two-path digital relaying systems: Detrimental or beneficial?" *IEEE Trans. Wireless Commun.*, vol. 10, no. 8, pp. 2468–2473, Aug. 2011.
[8] Y. Gong, C. Luo, and Z. Chen, "Two-path successive relaying with hybrid demodulate and forward," *IEEE Trans. Veh. Technol.*, vol. 61, no. 5, pp. 2044–2053, Jun. 2012.
[9] Y. Fan, C. Wang, J. Thompson, and H. V. Poor, "Recovering multiplexing loss through successive relaying using repetition coding," *IEEE Trans. Wireless Commun.*, vol. 6, no. 12, pp. 4484–4493, Dec. 2007.
[10] T. Wang and G. B. Giannakis, "High-throughput cooperative communications with complex field network coding," in *Proc. 41st Annu. Int. Conf. Inf. Sci. Syst.*, Mar. 14–16, 2007, pp. 253–258.
[11] H. Lu, P. Hong, and K. Xue, "High-throughput cooperative communication with interference cancellation for two-path relay in multi-source system," *IEEE Trans. Wireless Commun.*, vol. 12, no. 10, pp. 4840–4851, Oct. 2013.
[12] S. Zhang, S. C. Liew, and P. P. Lam, "Hot topic: Physical-layer network noding," in *Proc. Int. Conf. Mobile Comput. Netw.*, Sep. 23–26, 2006, pp. 358–365.
[13] R. E. Ziemer and R. L. Peterson, *Introduction to Digital Communication*. New York, NY, USA: Macmillan, 1992.
[14] J. G. Proakis, *Digital Communications*, 3rd ed. New York, NY, USA: McGraw-Hill, 1993.

Performance Analysis of Two-Way AF MIMO Relaying of OSTBCs With Imperfect Channel Gains

Arti M.K., *Student Member, IEEE*, and
Manav R. Bhatnagar, *Senior Member, IEEE*

***Abstract*—In this paper, we consider the relaying of orthogonal space–time block codes (OSTBCs) in a two-way amplify-and-forward (AF) multiple-input–multiple-output (MIMO) relay system with estimated channel state information (CSI). A simple four-phase protocol is used for training and OSTBC data transmission. Decoding of OSTBC data at a user terminal is performed by replacing the exact CSI by the estimated CSI in a maximum-likelihood (ML) decoder. Tight approximations for the moment-generating function (MGF) of the received signal-to-noise ratio (SNR) at a user is derived under Rayleigh fading by ignoring the higher order noise terms. Analytical average error performance of the considered cooperative scheme is derived by using the MGF expression. Moreover, the analytical diversity order of the considered scheme is also obtained for certain system configurations. It is shown by simulations and analysis that the channel estimation does not affect the diversity order of the OSTBC-based two-way AF MIMO relay system.**

***Index Terms*—Amplify-and-forward (AF) protocol, channel estimation, cooperative diversity, M-ary phase-shift keying (M-PSK), multiple-input–multiple-output (MIMO) system, orthogonal space-time block codes (OSTBCs), Rayleigh fading, symbol error rate (SER), two-way relaying.**

Manuscript received March 7, 2013; revised October 16, 2013; accepted February 1, 2014. Date of publication February 26, 2014; date of current version October 14, 2014. The review of this paper was coordinated by Prof. M. Uysal.

The authors are with the Department of Electrical Engineering, Indian Institute of Technology Delhi, New Delhi 110 016, India (e-mail: arti.mk@ee.iitd.ac.in; manav@ee.iitd.ac.in).

Color versions of one or more of the figures in this paper are available online at http://ieeexplore.ieee.org.

Digital Object Identifier 10.1109/TVT.2014.2308638